Extremely efficient host selectivity behaviour of stable di-(9-(*p*-chlorophenyl)xanthen-9-yl) peroxide towards *ortho*-xylene when crystallized from mixtures of the C_8H_{10} aromatic fraction of crude oil

Jarryd A. Vorgers,* Benita Barton, and Eric C. Hosten[a]

Department of Chemistry, PO Box 77000, Nelson Mandela University, Port Elizabeth, 6031, South Africa. E-mail: S219615039@mandela.ac.za

NELSON MANDELA UNIVERSITY

Introduction

Supramolecular chemistry is widely applied in areas such as the selective separation of positional isomers. In this study, the peroxide host compound **H** was investigated for its potential to separate mixtures containing xylene isomers (Xy) and ethylbenzene (EB) (Scheme 1). Complexes obtained during the study were characterized using NMR spectroscopy, gas chromatography, single-crystal X-ray diffraction (SCXRD) and thermal analysis techniques. Additionally, detailed guest–guest competition studies involving both equimolar and non-equimolar mixtures were undertaken, and the findings from these experiments are discussed herein. The separation of xylene isomers and ethylbenzene remains a considerable industrial challenge because these compounds possess very similar physical properties, particularly closely related boiling points within the range 136–144 °C. As a result, traditional fractional distillation methods require substantial energy input and result in high operational costs, motivating the search for alternative separation strategies such as host–guest inclusion chemistry.[1-3]

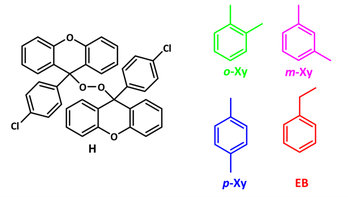

Scheme 1: Structures of host compounds **H** and EB and xylene guest compounds

Experimental

Synthesis of di-(9-(p-chlorophenyl)xanthen-9-yl) peroxide (H). Di-(9-(*p*-chlorophenyl)xanthen-9-yl) peroxide (**H**), the suggested host compound, was made in accordance with Taljaard's earlier work.[4,5]

Single solvent complexes: By dissolving the host molecule in different guest solvents, analysing the resulting crystals using GC, and obtaining overall H:G ratios using ^{1}H-NMR spectroscopy, the study examined the complexation ability of **H** for each of Xy/EB.

Equimolar mixed guest competition experiments. By dissolving the host molecule in different guest mixtures, analysing the resulting crystals using GC, and obtaining overall H:G ratios using ^{1}H-NMR spectroscopy, the study examined the selectivity of **H** in mixed Xy/EB. Every experiment was carried out twice, and percentage estimated standard deviations are given for each.

Binary guest competition experiments in which the quantity of each guest was varied. H was dissolved in binary Xy/EB solutions with different molar ratios of Guest A and Guest B, the resulting crystals were analysed by GC, and selectivity plots were constructed using the equation suggested by Pivovar et al. [6]

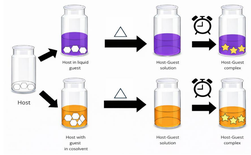

Figure 1. Experimental procedure for host-guest complex formation.

Results

Table 1 Results from the equimolar mixed Xy/EB guest experiments with **H**

o-Xy	*m*-Xy	*p*-Xy	EB	Guest ratios	Overall H : G ratios	% e.s.d.s
X	X			**90.4** : 9.6	1 : 1	1.9
X		X		**81.9** : 18.1	2 : 3	0.6
X			X	**95.3** : 4.7	1 : 1	0.9
	X	X		*b*	*b*	*b*
	X		X	*b*	*b*	*b*
		X	X	*b*	*b*	*b*
X	X	X		*b*	*b*	*b*
X	X		X	*b*	*b*	*b*
X		X	X	*b*	*b*	*b*
	X	X	X	*b*	*b*	*b*
X	X	X	X	**74.4** : 7.4 : 13.9 : 4.3	2 : 1	0.6 : 0.3 : 0.7 : 1.1

[a] Guest and overall H : G ratios were obtained through GC and ^{1}H-NMR experiments, respectively. [b] No guest solvent was detected in the solids emanating from these experiments.

Table 2 Selectivity coefficients for the data points contained in the selectivity profiles[a]

o-Xy percentage in the original solution	*K* values (in favour of) *o*-Xy/*m*-Xy	*o*-Xy/*p*-Xy	*o*-Xy/EB
20	13.9 (*o*-Xy)	9.3 (*o*-Xy)	1.2 (*o*-Xy)
40	13.4 (*o*-Xy)	7.7 (*o*-Xy)	33.5 (*o*-Xy)
50	9.4 (*o*-Xy)	4.5 (*o*-Xy)	20.3 (*o*-Xy)
60	7.4 (*o*-Xy)	4.5 (*o*-Xy)	23.9 (*o*-Xy)
80	3.9 (*o*-Xy)	2.7 (*o*-Xy)	9.8 (*o*-Xy)

[a]Guests in brackets after the *K* values are those preferred in that particular experiment.

It was determined that in single solvent experiments that **H** possessed host ability for *o*- and *p*-Xy and therefore mixed guest crystallization experiments were feasible in order to ascertain whether **H** is selective in such conditions. Table 1 summarises the results that were obtained when **H** was crystallized from the various equimolar mixtures of these isomers.

Only the binary guest combinations which contained *o*-Xy furnished complexes, with all of the other binary mixtures affording guest-free host compound only. The selectivity coefficients for all data points contained in these plots are summarised in Table 2, with those approaching 10 or greater implying that these binary solutions in particular may be separated by means of supramolecular chemistry protocols. The *K* values for the equimolar binary experiments from Table 1 have been calculated here as well (Table 2).[7]

Crystals emanating from the 20, 40, 60 and 80% *o*-Xy/ *m*-Xy mixtures contained 77.6, 89.9, 91.7 and 94.0% *o*-Xy. The *K* values that were calculated for these experiments ranged between 3.9 and 13.9 (Table 2). Two solutions may be separated using this strategy, those containing 20 and 40% *o*-Xy; *K* measured 13.9 and 13.4, respectively. In the remaining two solutions, the 60 and 80% *o*-Xy experiments, separations are not feasible owing to these experiments being characterised by low *K* values, 7.4 and 3.9. Furthermore, *K* was 9.4 for the 50% *o*-Xy experiment, and this too cannot be separated in this particular fashion.

o-Xy/*p*-Xy experiments, once more, demonstrated that **H** remained consistently selective for *o*-Xy though, it must be said, this host affinity behaviour was somewhat lower than in the *o*-Xy/*m*-Xy experiments. The 20, 40, 60 and 80 *o*-Xy mixtures furnished complexes with 69.9, 83.7, 87.0 and 91.4% *o*-Xy. In each case, the calculated *K* value was too low (2.7–9.3) to present **H** as a possible host candidate for efficient separations of these solutions. This was also the case for the 50% *o*-Xy solution where *K* was calculated to be only 4.5. Remarkable observations are evident from the *o*-Xy/EBexperiments. While the 20% *o*-Xy solution afforded a complex with only slightly elevated quantities of *o*-Xy (22.7%, *K* = 1.2), the remaining experiments saw a near-complete encapsulation of this guest species. From the 40, 60 and 80% *o*-Xy solutions crystallized complexes with as much as 95.7, 97.3 and 97.5% *o*-Xy. In the first two of these, *K* was extraordinary, 33.5 and 23.9, while in the last experiment (80% *o*-Xy), *K* approached 10 (9.8). Additionally, *K* was determined to be 20.3 for the 50% *o*-Xy experiment. Therefore, in all cases, with the exception of the 20% *o*-Xy solution, **H** would be an extremely effective host compound for such separations/purifications.

Results continued

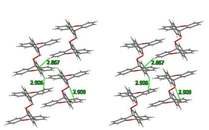

Figure 2 A stereoview of the intra- and intermolecular C–H···π interactions in guest-free **H**

Figure 3 The intermolecular π···π close contacts in guest-free **H**

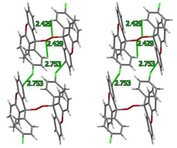

Figure 4 A stereoview of the weak nonclassical C–H···Cl (intermolecular) and C–H···O (intramolecular) interactions present in guest-free **H**

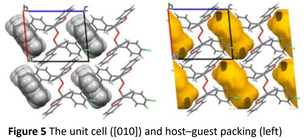

Figure 5 The unit cell ([010]) and host–guest packing (left) and voids (right) in **H**·*o*-Xy. Guest and host molecules are in spacefill and stick representations, respectively

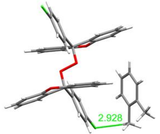

Figure 6 (Guest)H$_2$C–H···Cl–C(host) interaction in the complex with *o*-Xy

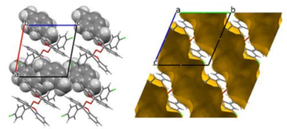

Figure 7 Host–guest packing (left) and voids (right) in **H**·2(*p*-Xy). Guest and host molecules are in spacefill and stick forms, respectively

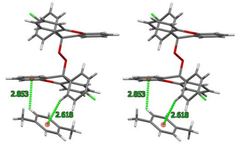

Figure 8 Two of the three C–H···π contacts present in **H**·2(*p*-Xy)

The molecular geometry of the host species was observed to possess an inversion centre in the midpoint of the O–O peroxide functionality. This geometry (figure 2, a stereoview) was maintained by means of an intramolecular C–H···π interaction (2.91 (H···π) and 3.836(2) (C···π) Å, 165°), whilst the packing was stabilized by a series of intermolecular interactions (Figure 2 , 2.87 and 2.91, 3.699(2) and 3.723(2) Å, 147 and 145°, respectively) of this kind and, additionally, intermolecular π···π close contacts as demonstrated in Figure 3 (3.708(1) and 3.887(1) Å, with slippages of 1.198 and 1.990 Å).

Two weak hydrogen bonds were also identified in this crystalline solid, one intermolecular and the other intramolecular in nature. In the first of these were involved an aromatic hydrogen atom on the xanthenyl system and a chlorine atom on the free aromatic ring. Measurements were 2.75 (H···Cl) and 3.646(2) Å (C···Cl), and the bond angle was 157°. This is illustrated in Figure 4 (a stereoview) together with the intramolecular close contact between an aromatic hydrogen atom on the free aromatic moiety and an oxygen atom of the peroxide functional group (2.43 (H···O) and 2.774(2) (C···O) Å, 101°).

The unit cell and host–guest packing in complex **H**·*o*-Xy is illustrated in Figure 5 (left), while the void diagram after deleting the guest molecules from the packing calculation may be viewed on the right-hand side. These guest molecules occupied discrete cavities in the crystalline complex.

A singular intermolecular π···π interaction was observed between host molecules in this complex, together with one (host)C–H···π(host) close contact. Applicable measurements were 3.9792(10) Å (slippage 0.861 Å), and 2.95 and 3.7883(18) Å (148°). The guest molecule did not interact in this manner. Additionally, nonclassical hydrogen bonds were evident and involved a hydrogen atom of the free aromatic moiety and the oxygen of the peroxide group within the same molecule (2.46, 2.8124(16) Å, 102°), as well as another hydrogen on the free ring and the xanthenyl oxygen atom of a neighbouring host molecule (2.53, 3.392(2) Å, 151°). The guest molecules were also retained in the complex by means of nonclassical hydrogen bonds: here, a hydrogen atom of the methyl group of *o*-Xy interacted favourably with the host chlorine atom (Figure 6). Measurements were 2.93 Å and 155°. This was the only host···guest close contact identified in this complex.

A singular intermolecular π···π interaction was observed between host molecules in this complex, together with one (host)C–H···π(host) close contact. Applicable measurements were 3.9792(10) Å (slippage 0.861 Å), and 2.95 and 3.7883(18) Å (148°). The guest molecule did not interact in this manner. Additionally, nonclassical hydrogen bonds were evident and involved a hydrogen atom of the free aromatic moiety and the oxygen of the peroxide group within the same molecule (2.46, 2.8124(16) Å, 102°), as well as another hydrogen on the free ring and the xanthenyl oxygen atom of a neighbouring host molecule (2.53, 3.392(2) Å, 151°). The guest molecules were also retained in the complex by means of nonclassical hydrogen bonds: here, a hydrogen atom of the methyl group of *o*-Xy interacted favourably with the host chlorine atom (Figure 6). Measurements were 2.93 Å and 155°. This was the only host···guest close contact identified in this complex.

Figure 7 (left, [010]) depicts the host–guest packing and unit cell, and the voids (right, [100]) for the complex containing *p*-Xy. Note that while the ^{1}H-NMR experiment suggested a 4:1 H:G ratio, this was observed to be 1:2 through SCXRD analysis. The discrepancy in these ratios is as a result of the extreme instability of this complex, as will be discussed in the Thermal analysis section.

Interestingly, the guest molecules in this complex resided in infinite channels rather than discrete cavities as was the case for *o*-Xy. This observation explains the affinity of **H** for *o*-Xy in the guest competition experiments: channel occupation by guest molecules is associated with decreased thermal stabilities of inclusion compounds while complexes in which guests are accommodated in discrete cavities are usually more stable (the thermal stability of the two complexes of the present investigation are reported in the Thermal analysis section that follows).

A scrutiny of the noncovalent interactions present in **H**·2(*p*-Xy) was subsequently undertaken. While no π···π interactions could be identified, the guest molecule experienced two (host)C–H···π(guest) close contacts involving both the host xanthenyl and free aromatic hydrogen atoms. Applicable measurements were 2.84 and 3.512(2) Å (129°), and 2.62 and 3.498(2) Å (154°). Furthermore, a (guest)C–H···π(host) interaction was also identified (2.85, 3.486(2) Å, with a bond angle of 125°). Two of these three interactions are depicted in Figure 8(a stereoview). Moreover, no nonclassical hydrogen bonds between the host and guest species (and, also, between host and host molecules) were noted in this complex (contrarily to the guest in **H**-*o*-Xy, which did interact in this manner with the host species); this observation may, together with the type of guest accommodation already discussed (discrete cavities *vs.* channels), provide a plausible reason for the host selectivity for the *ortho* isomer rather than *p*-Xy in the guest competition experiments.

Results continued

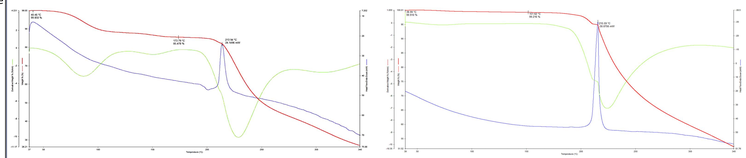

Figure 9 The DSC (blue), TG (red) and DTG (green) traces for (a) H·*o*-Xy and (b) 4(H)·*p*-Xy.

The thermal traces that were obtained after thermal analysis on the two complexes produced in this work are provided in Figure 9a and b. Here, the differential scanning calorimetric (DSC), thermogravimetric (TG) and its derivative (DTG) curves are overlaid in each one. The temperature at which the guest release event initiates (T_{on}) serves as a measure of the relative thermal stabilities for these complexes; these are summarised in Table 3 together with the experimental and expected mass losses, and the endotherm peak temperature (T_p) representing the decomposition of **H**.

The guest species in the complex **H**·*o*-Xy, upon being subjected to the heating program in this thermal experiment, escaped from the discrete cavities of the complex in two broad steps (Figure 9a). T_{on} was 40.5 °C (Table 3). The measured and expected mass losses concurred closely (14.4 *vs.* 14.7%). However, a consideration of these traces for the *p*-Xy inclusion compound Figure 9b) revealed extreme instability at ambient conditions. Only 0.7% of the guest was observed to be lost in this experiment (the expected mass loss was 4.1%), with most of the release event occurring during sample preparation. T_{on} could also, as a consequence, not be measured. This observation is not entirely unexpected given the fact that *p*-Xy was accommodated in wide open channels in the crystals which facilitates facile guest escape (while the guest in **H**·*o*-Xy experienced discrete cavity occupation and was, as a result, more stable). Therefore, the preferred guest of **H** in the guest competition experiments, *o*-Xy, formed a complex that was significantly more stable than that containing the *para* isomer, a guest not favoured by **H**. These observations, once more, explain the selectivity behaviour of this host compound when presented with mixed guest solutions.

Table 3 Thermal parameters obtained from the thermal traces

Complex	T_{on} (°C)	Measured mass loss (%)	Expected mass loss (%)
H·*o*-Xy	40.5 °C	14.4%	14.7%
4(**H**)·*p*-Xy	Could not be determined due to early guest release	Could not be determined due to early guest release	4.1%

[a]T_{on} is the temperature at which the guest release process commenced and represents the relative thermal stability of the complex, while T_p is the endotherm peak temperature representing the host decomposition event. [b]This complex was unstable at ambient conditions.

Conclusion

Di-(9-(*p*-chlorophenyl)xanthen-9-yl) peroxide (**H**) exhibited selective inclusion behaviour toward aromatic isomers. Crystallization experiments showed that H formed inclusion compounds with *o*-xylene and *p*-xylene, while *m*-xylene and ethylbenzene produced only the guest-free host. Guest competition experiments demonstrated a strong preference for *o*-xylene, with significant selectivity coefficients obtained for several *o*-xylene/*m*-xylene and *o*-xylene/ethylbenzene mixtures.

SCXRD analysis revealed that *o*-xylene was accommodated within discrete cavity voids, whereas *p*-xylene occupied wide open channels within the crystal lattice. The preferred *o*-xylene guest also formed stabilizing non-classical hydrogen-bonding interactions with the host. Thermal analysis showed that the **H**-*o*-Xy complex was considerably more stable than the **H**·2(*p*-Xy) complex, consistent with the different guest voids.

These findings demonstrate the potential of **H** as a more selective and greener alternative for the separation of xylene isomers and ethylbenzene, which are traditionally difficult to separate by fractional distillation due to their similar physicochemical properties.

References

(1) Barton, B.; Senekal, U.; Hosten, E. C. Compounds N,N'-Bis(9-Cyclohexyl-9-Xanthenyl)Ethylenediamine and Its Thio Derivative, N,N'-Bis(9-Cyclohexyl-9-Thioxanthenyl)Ethylenediamine, as Potential Hosts in the Presence of Xylenes and Ethylbenzene: Conformational Analyses and Molecular Modelling Considerations. Tetrahedron 2019, 75 (25), 3399–3412. https://doi.org/10.1016/j.tet.2019.04.065.

(2) Nassimbeni, L. R.; Báthori, N. B.; Patel, L. D.; Su, H.; Weber, E. Separation of Xylenes by Enclathration. Chemical Communications 2015, 51 (17), 3627–3629. https://doi.org/10.1039/c4cc05329g.

(3) Mohameed, H. A.; Jdayil, B. A.; Takrouri, K. Separation of Para-Xylene from Xylene Mixture via Crystallization. Chemical Engineering and Processing: Process Intensification 2007, 46 (1), 25–36. https://doi.org/10.1016/j.cep.2006.04.002.

(4) Taljaard, B. The Synthesis and Reactions of Stable Peroxides , university of Port Elizabeth, Port Elizabeth, 1986.

(5) Glover, S. A.; Goosen, A.; McCleland, C. W.; Taljaard, B.; Ruric Vogel, F.; Goosen, A.; McCletand, C.; Taljaaroand Vogel, B. F. Stable Hydroperoxide Synthesis. *S. Afr. J. Chem* 1984, 164–170.

(6) Pivovar, A. M.; Holman, K. T.; Ward, M. D. Shape-Selective Separation of Molecular Isomers with Tunable Hydrogen-Bonded Host Frameworks. *Chemistry of Materials* 2001, *13* (9), 3018–3031. https://doi.org/10.1021/cm010445z.

(7) Nassimbeni, L. R.; Sykes, N. M. Inclusion Compounds: Structure, Kinetics and Selectivity. *Crystallogr Rev* 2022, No. May. https://doi.org/10.1080/0889311X.2022.2067849.